Dynamics of electronic transport in metal/organic/metal structures

1999 J. Phys.: Condens. Matter 11 L7

(http://iopscience.iop.org/0953-8984/11/2/001)

J. Phys.: Condens. Matter **11** (1999) L7–L14. Printed in the UK PII: S0953-8984(99)98989-0

LETTER TO THE EDITOR

Dynamics of electronic transport in metal/organic/metal structures

Z G Yu, D L Smith, A Saxena and A R Bishop
Los Alamos National Laboratory, Los Alamos, New Mexico 87545, USA

Received 3 November 1998

Abstract. We develop a novel self-consistent Green's function approach to study the dynamics of electronic transport across a metal/conjugated–oligomer/metal structure. We find a crossover behaviour in transport from free electron to polaron-like, with increasing phonon frequency of the oligomer. In the former, lattice motion lags behind the wavepacket of an incoming electron; whereas, in the latter, the lattice can follow the electron. To simulate lattice fluctuations we study a pre-existing lattice distortion and find enhanced sub-gap transmission. These results have implications for transport experiments on polymer light-emitting diodes and molecular wires.

The study of electronic transport across organic tunnel devices, e.g. metal/conjugated–oligomer/metal structures, has recently become important both due to their technological applications and for a fundamental understanding of competing time scales in electron–lattice coupled systems. Examples of such devices include polymer light-emitting diodes (PLEDs) [1] and molecular wires sandwiched either between metals or a metal and an STM tip [2, 3, 4, 5]. Conjugated oligomers in these devices are quite different from inorganic semiconductors in that oligomers are flexible and have strong electron–lattice interactions. Thus polaron formation and lattice fluctuations are expected to crucially affect the transport properties in the organic tunnelling device, which make it quite distinct from inorganic semiconductor double barrier tunnelling structures. In the context of conjugated polymers and PLEDs, polarons are usually assumed to be the primary charge carriers [6]. In contrast, the oligomer in a molecular wire [7, 8, 9] is frequently treated as a rigid lattice, with the carriers assumed to be free electrons. These assumptions with regard to the nature of carriers in these organic structures are not obviously justified. Since the electronic and lattice motions influence each other, they must be treated self-consistently. This is an intrinsically dynamical problem but, due to the complexity and numerical intensity of the dynamical calculations, only static calculations have been carried out to date [7, 8, 9, 10].

To address these basic issues we develop here a physically appealing Green's function dynamical formalism, which treats the electronic and lattice time evolution self-consistently, and is applicable to a variety of device configurations. We find the following major results. (i) The carrier transport behaviour depends on the ratio of the electronic time scale and the lattice time scale (phonon period). Both free electron and polaron limiting behaviour can be realized in these structures by tuning the phonon frequency of the oligomer for fixed electronic parameters. (ii) In the low-frequency regime, the lattice responds to the incoming electron slowly and lags behind the electron, so that the carrier is basically a free electron; whereas in the high-frequency regime, the lattice can follow the electron motion, and the carrier is polaron-like

0953-8984/99/020007+08$19.50

(i.e., electron dressed with a lattice distortion). (iii) Lattice fluctuations are important in certain circumstances and they can produce a transient polaron-like or soliton-like lattice distortion, which qualitatively changes the transmission of the incoming electron.

Several recent experiments have observed the lattice effects on electronic conduction through organic molecular wires and photoelectron transmission through organic thin films [11, 12]. We present the *first* dynamical simulation of electronic transport in *organic* sandwich structures. Our results have wide applicability to these and related problems and to the interpretation of experiments in molecular electronic structures with metal/organic interfaces, such as conjugated self-assembled monolayer spacers to control electron injection, single electron organic transistors, etc. Furthermore, our dynamical approach can be used to determine to what extent the usual rigid lattice assumption of transport in quantum wires is valid, and when lattice dynamics must be self-consistently employed for a proper understanding of the transport.

We consider an oligomer chain with N atoms sandwiched between two semi-infinite metal leads. The total Hamiltonian of this system consists of three parts $H = H_{\rm met} + H_{\rm oli} + H_{\rm int}$. We describe the metal by a one-dimensional (1D) tight-binding model

$$H_{\rm met} = -t_0 \left[\sum_{l=-\infty}^{-1} (c_{l+1}^{\dagger} c_l + \text{H.c.}) + \sum_{l=N+1}^{\infty} (c_{l+1}^{\dagger} c_l + \text{H.c.}) \right]$$

and the oligomer by the Su–Schrieffer–Heeger (SSH) model for *trans*-polyacetylene [13]

$$H_{\rm oli} = -\sum_{l=1}^{N-1} [t - \alpha \Delta_l](c_{l+1}^{\dagger} c_l + \text{H.c.}) + \sum_{l=1}^{N-1} \frac{K}{2} \Delta_l^2 + \sum_{l=2}^{N-1} \frac{p_l^2}{2M}.$$

Here $c_l^{\dagger}$ (c_l) is the electron creation (annihilation) operator at site l, $\Delta_l = u_{l+1} - u_l$, u_l (p_l) the lattice displacement (momentum) of the lth atom, α the electron–lattice coupling, M the atom mass and K the spring constant. The positions of the atoms in the metal leads and the oligomer atoms at site 1 and N are taken to be fixed. The interface coupling between metals and the oligomer is through hopping $H_{\rm int} = -t_1(c_1^{\dagger} c_0 + c_{N+1}^{\dagger} c_N + \text{H.c.})$. The idealized 1D contacts and metals enable us to efficiently capture main qualitative features, which depend weakly on the detailed structure of contacts [10]. We study this model by explicitly taking into account all valence electrons in the oligomer and electrons below the Fermi energy of the metal.

We determine the initial lattice configuration of the oligomer in the ground state after it is attached to metal leads by requiring $\delta\langle H\rangle/\delta u_l = 0$. The interface coupling $H_{\rm int}$ causes an energy change compared with the isolated oligomer and metals, which can be calculated by

$$\delta\mathcal{E} = \int_{-2t_0}^{E_F} \mathrm{d}E\, E \delta\rho(E)$$

where E_F is the Fermi energy of the metal, $\delta\rho$ is the change of density of states, and we obtain

$$\delta\rho(E) = -\frac{1}{\pi} \mathrm{Im} \frac{\mathrm{d}}{\mathrm{d}E} \left[\ln(1 - t_1^2 \tilde{G}_{00} \tilde{G}_{11}) + \ln(1 - t_1^2 \tilde{G}_{NN} \tilde{G}_{N+1N+1}) \right].$$

Here $\tilde{G}_{ll'}(E)$ is the Green's function for $H_{\rm oli} + H_{\rm met}$, which is defined by $\tilde{G}_{ll}(E) = \sum_i |\langle l|\phi_i\rangle|^2/(E - E_i + \mathrm{i}\epsilon)$, where ϕ_i is the eigenfunction of the ith level in the metal or the oligomer, depending on whether l is in the metal or the oligomer, and E_i its energy. The detailed derivation and expressions for $\delta\rho(E)$ and $\tilde{G}_{ll'}(E)$ will be presented elsewhere. Thus $\delta\langle H\rangle/\delta u_l$ contains two parts, $\delta\langle H\rangle/\delta u_l = \delta\langle H_{\rm oli}\rangle/\delta u_l + \delta\mathcal{E}/\delta u_l$. We regard $H_{\rm int}$ as the interacting part of the total Hamiltonian and the very short-range potential of $H_{\rm int}$ enables us to treat it rigorously rather than perturbatively.

We construct a wavepacket far from the interface at the left metal to study dynamics of electronic transport across this sandwich device. We take the wavepacket initially to have a Gaussian profile

$$\psi_l(\tau_0) = C \exp\left[ik_0(l-l_0) - \frac{(l-l_0)^2}{4(\delta l)^2}\right]$$

where k_0 is the mean momentum of this wavepacket, l_0 its location, and δl its width.† Denoting $H_0 = H_{\rm met} + H_{\rm oli}$, we study the evolution of the incoming electron by solving the time-dependent Schrödinger equation for the wavepacket $(i\hbar\partial/\partial\tau - H_0)\psi_l(\tau) = H_{\rm int}\psi_l(\tau)$. Because of strong electron–lattice coupling in the oligomer, the lattice and wavepacket motions influence each other and must be determined self-consistently. We determine the lattice configuration of the oligomer by solving the classical lattice equation of motion $M{\rm d}^2u_l/{\rm d}\tau^2 = -\delta\langle H\rangle/\delta u_l$.

For a given lattice configuration at time τ, we calculate the electronic Green's function of H_0 using $G_{ll'}(\delta\tau,\tau) \equiv -i\langle l|\exp[-iH_0(\tau)\delta\tau/\hbar]|l'\rangle$. For the left metal ($-\infty < l, l' \leqslant 0$), we obtain $G_{ll'}(\delta\tau;\tau) = -i[i^{|l-l'|}J_{|l-l'|}(\gamma\delta\tau) - i^{|l+l'-2|}J_{|l+l'-2|}(\gamma\delta\tau)]$ with $\gamma \equiv 2t_0/\hbar$, and $J_l(x)$ the lth order Bessel function of the first kind. The expression for the right metal is similar. For the oligomer $(1 \leqslant l, l' \leqslant N)$ $G_{ll'}(\delta\tau;\tau) = -i\sum_i \langle l|\phi_i(\tau)\rangle\langle\phi_i(\tau)|l'\rangle e^{-iE_i\delta\tau/\hbar}$. So after a small time interval $\delta\tau$ (0.01 fs in our numerical calculations for reliable results), the wavefunction of the wavepacket is obtained through the iteration equation

$$\Psi(\tau+\delta\tau) = i\mathcal{G}(\delta\tau;\tau)\Psi(\tau) + \mathcal{S}(\delta\tau;\tau)H_{\rm int}\Psi(\tau)$$

where $\mathcal{G}$ is the Green's function matrix and $S_{ll'}(\delta\tau,\tau) = \int_0^{\delta\tau} {\rm d}\tau' G_{ll'}(\delta\tau - \tau';\tau)/\hbar^2$. Since $H_{\rm int}$ is very localized (in real space nonzero elements of $H_{\rm int}$ form two 2×2 submatrices), the above equation essentially contains one summation. Thus our approach is efficient for studying the wavepacket evolution. Since both the metal and the oligomer are described by Green's functions, our approach can be easily extended to other metals and oligomers by using the Green's functions for these materials in the iteration equation.

The updated lattice configuration after time interval $\delta\tau$ is obtained from

$$u_l(\tau+\delta\tau) = u_l(\tau) + \frac{p_l(\tau)}{M}\delta\tau$$
$$p_l(\tau+\delta\tau) = p_l(\tau) + F(\tau)\delta\tau$$

where $F(\tau) \equiv -\delta\langle H\rangle/\delta u_l = -[\delta\langle H_{\rm oli}\rangle/\delta u_l + \delta\mathcal{E}/\delta u_l]$. Here, however, $\delta\langle H_{\rm oli}\rangle/\delta u_l$ should include the contribution of both valence electrons and the incoming wavepacket. The wavepacket contribution is $2\alpha[{\rm Re}(\psi^*_{l+1}(\tau)\psi_l(\tau)) - {\rm Re}(\psi^*_l(\tau)\psi_{l-1}(\tau))]$.

The transmission (T) and reflection (R) coefficients are computed by integrating currents over time at the left and right metals far from the interfaces. For the initial wavepacket normalized to unit incident current density

$$T = \int_{\tau_0}^{\infty} {\rm d}\tau j_r(\tau) \qquad R = \int_{\tau_0}^{\infty} {\rm d}\tau j_l(\tau)$$

where the currents are $j_r(\tau) = it_0(\psi^*_{l+1}\psi_l - \psi^*_l\psi_{l+1})$ $(l \gg N)$ and $j_l(\tau) = it_0(\psi^*_l\psi_{l+1} - \psi^*_{l+1}\psi_l)$ $(l \ll 0)$.

As an example, we study a sandwich structure with an 8-atom oligomer. We fix the width of the initial wavepacket, $\delta_l = 10$ lattice constants, and the Fermi energy of the metals, $E_F = 0$. The wavepacket width can be tuned to change the sharpness of the wavepacket energy distribution. Other parameters are $t_0 = 2.6$ eV, $t_1 = 1.5$ eV, $t = 2.5$ eV, $\alpha = 7$ eV Å^{-1} and

† We assume the energy of the incoming wavepacket is well above E_F to ensure the scattered states are unoccupied.

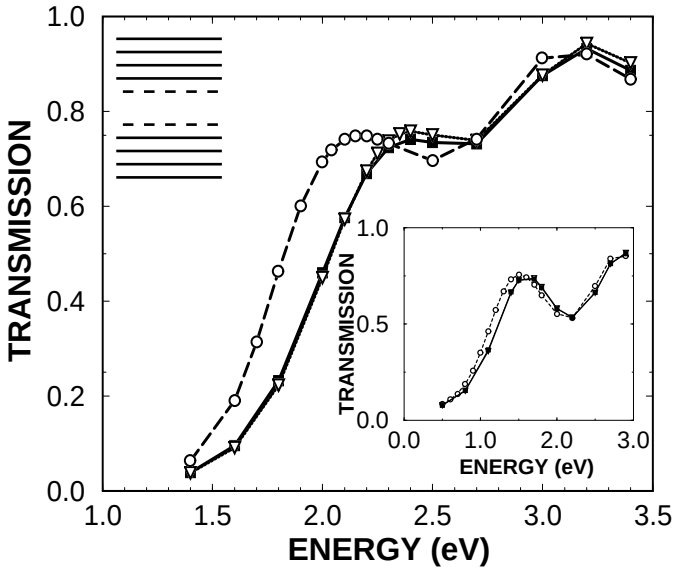

Figure 1. Electronic transmission as a function of the incoming wavepacket energy for $\alpha = 7$ eV Å^{-1}. The dotted (triangles), solid and dashed curves correspond to $\omega = 0$, $\omega = \omega_0$ and $\omega = 10\omega_0$. Upper inset shows schematic electronic levels of the oligomer; dotted curves denote polaron levels.

$K = 40$ eV Å^{-2}, which are typical values for conjugated linear polymers. Figure 1 shows the transmission coefficient as a function of the energy of the incoming wavepacket. With fixed electronic structure, we tune the bare optical phonon frequency $\omega = 2\sqrt{K/M}$ by changing the atomic mass M of the oligomer to systematically study the transport. The dotted line (triangles) is for the case $\omega = 0$, i.e., the lattice does not move and stays in the ground state configuration while the wavepacket tunnels through the oligomer. The transmission peaks come from resonant tunnelling, which occurs when the energy of the wavepacket coincides with discrete levels of the oligomer. These peaks are broad because of the finite width of the wavepacket. The solid line describes the case $\omega = \omega_0 = 0.2268$ eV, which is close to the value in *trans*-polyacetylene. We see from the figure that the transmission is essentially the same as that in the static case ($\omega = 0$). However, if the phonon frequency is large, e.g., $\omega = 10\omega_0$, as shown by the dashed line, the transmission is quite different from that in the static or low-frequency cases, especially in the region below the energy gap of the oligomer. The first resonant tunnelling peak shifts notably toward lower energy, and the transmission is enhanced below the gap. For a smaller $\alpha = 5.6$ eV Å^{-1}, as shown in the lower inset of figure 1, we observe a very similar behaviour of transmission as we change the phonon frequency. The only difference is that for smaller α the shift of the first peak is less pronounced.

To understand the different transmission behaviour in different phonon frequency regimes, we examine the charge density of the wavepacket and the magnitude of the lattice distortion from its equilibrium configuration in the oligomer for different times. Figure 2 illustrates the case in the low-frequency regime, $\omega = \omega_0$. The circles, squares and triangles correspond to $\tau = 6$, 8, 10 fs. Figure 2(a) shows that from 6 to 10 fs, the wavepacket is moving from the left interface to the right one. Because of the electron–lattice coupling, the lattice moves away from its equilibrium configuration, as shown in figure 2(b). However, during this period, the lattice is within its first oscillation period and lags behind the wavepacket motion. The

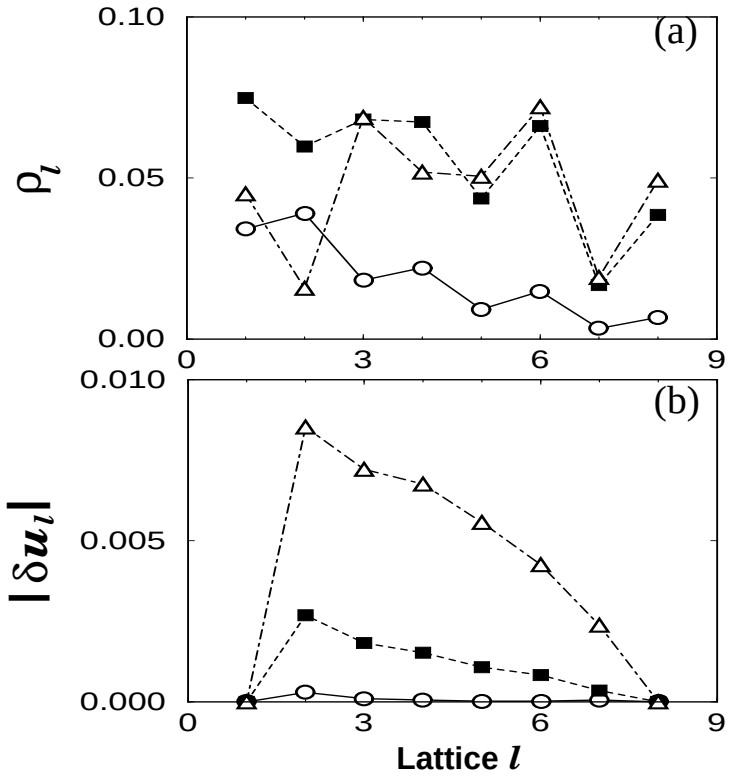

Figure 2. Snapshot of charge density of the wavepacket and magnitude of the lattice distortion in the oligomer for $\omega = \omega_0$. The circles, squares and triangles correspond to $\tau = 6$, 8, 10 fs. The energy of the incoming wavepacket is 2.1 eV.

wavepacket behaves like a free electron and the transmission is close to that of the static case.

The high-frequency $\omega = 10\omega_0$ results are shown in figure 3. The lattice behaviour is quite different from that in $\omega = \omega_0$. During the period from 6 to 10 fs, as the wavepacket moves from the left interface to the right one, the profile of the lattice distortion also moves through the oligomer, following the wavepacket motion. Now the carrier is not a free electron but the electron is surrounded by a localized lattice distortion, in a polaron-like cloud. Therefore, in the high-frequency regime, the first transmission peak shifts toward the polaron electronic level which lies below the energy gap, as shown in figure 1. We also find the crossover from the free electron-like to polaron-like behaviour by tuning the electronic time scale with a fixed physically realistic phonon frequency of the oligomer ($\omega = \omega_0$). The electronic time scale is determined by the momentum of the incoming wavepacket, $\hbar/|2t_0 \sin k|$ for the dispersion $E_k = E_0 - 2t_0 \cos k$ of the metal. We have chosen different site energy E_0 of the metal so that the wavepacket can have different momenta for the same energy. Thus, whether the carrier is like a free electron or a polaron depends on the ratio between the electron time scale and the lattice time scale.

Although, from the above calculations, it seems that polaron effects are not extremely important in typical polymers, strong lattice fluctuations may change this picture dramatically. Due to the low dimensionality of polymers, lattice fluctuations can be sufficiently strong to produce some transient soliton- or polaron-like lattice distortion. Since the polaron configuration has the most important contribution to lattice fluctuations in oligomers, we

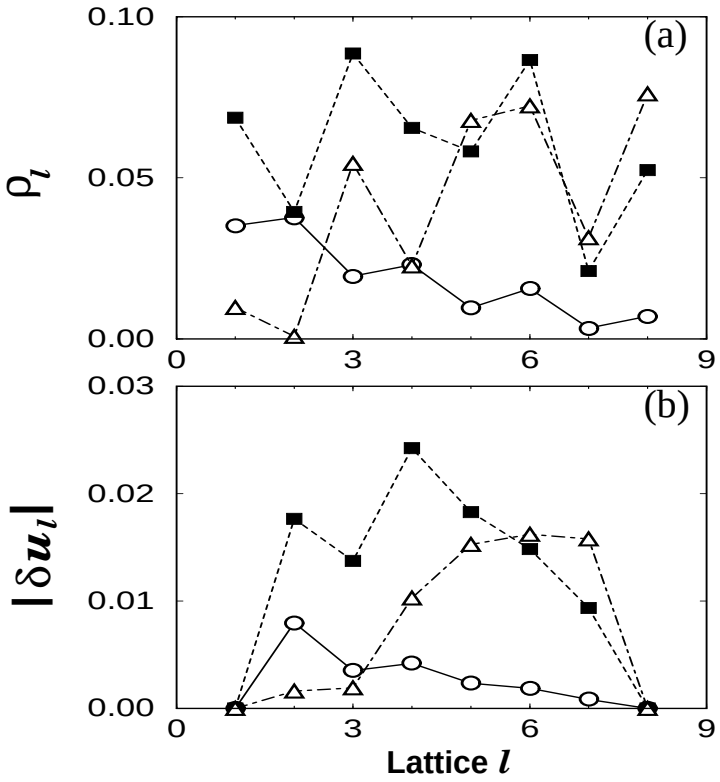

Figure 3. Snapshot of charge density of the wavepacket and magnitude of the lattice distortion in the oligomer for $\omega = 10\omega_0$. The symbols and the energy of wavepacket are the same as in figure 2.

assume a pre-existing polaron lattice distortion and calculate the wavepacket transmission to study fluctuation effects. In figure 4, we show the transmission as a function of the energy of the incoming wavepacket with a pre-existing polaron-like lattice distortion. The dashed and dot-dashed lines correspond to $\omega = 0$ and $\omega = \omega_0$. For $\omega = 0$, because the lattice does not move, the first resonant tunnelling peak is from the polaron level in the oligomer. For $\omega = \omega_0$, although the first transmission peak shifts from the polaron level toward higher energy compared to the case of $\omega = 0$, it is still much lower than the energy gap (first peak of the solid line). This indicates that the wavepacket can use a 'partially formed' polaron level produced by lattice fluctuations to tunnel through the oligomer, although the carrier behaviour here is more like a free electron. Thus polaron effects may be important even in the low-frequency regime due to the presence of strong lattice fluctuations in oligomers. The present realization of lattice fluctuations is more realistic compared to the previous approximation treated as static disorder [10]. The sub-gap transmission is enhanced in both cases, although at somewhat different energies.

In summary, because of strong electron–lattice coupling in organics, the electronic and lattice time evolutions should be calculated self-consistently. To this end, we have developed an efficient and physically intuitive Green's function approach to study the dynamics of wavepacket tunnelling through organic sandwich structures. The approach can be easily extended to other configurations. We found a crossover behaviour in transport with increasing phonon frequency of the oligomer. In the low-frequency regime, the lattice motion lags

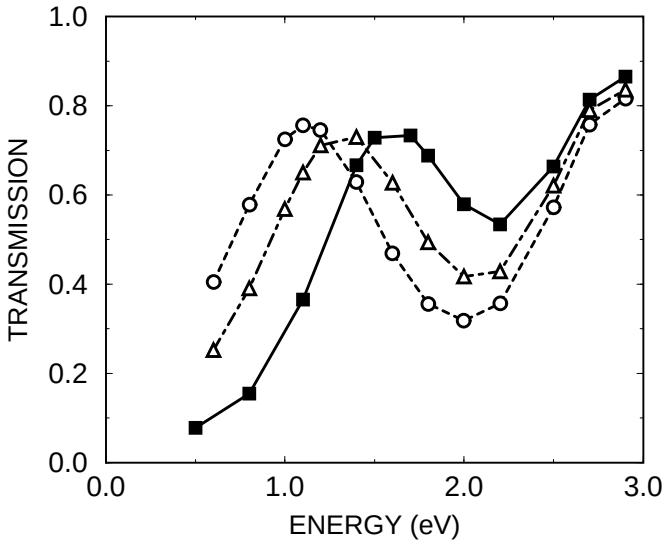

Figure 4. Electronic transmission as a function of the incoming wavepacket energy with a pre-existing polaron-like lattice distortion. The electron–lattice coupling is $\alpha = 5.6$ eV/Å. Dashed and dot-dashed curves correspond to $\omega = 0$ and $\omega = \omega_0$. The solid line is for reference purposes, obtained by using the equilibrium lattice configuration and $\omega = \omega_0$.

behind the wavepacket of the incoming electron and the transmission is very close to that in the static case. The carrier in this regime is like a free electron as in inorganic sandwich devices. In contrast, in the high-frequency regime, the lattice can follow the motion of the injected electron and the carrier is like a polaron. Thus the first resonant tunnelling peak in transmission shifts toward the polaron energy level of the oligomer. We calculated the dynamical electronic transmission with a pre-existing lattice distortion to simulate lattice fluctuations. Strong lattice fluctuations in 1D oligomers may lead to transient polaron-like lattice distortions, which change the transmission of these tunnel structures substantially, even in the low phonon frequency regime. Our microscopic results should provide valuable input to macroscopic device models, e.g. cross-sections for scattering events and carrier mobilities.

This work was supported by the LDRD/MEEM program at LANL and the US Department of Energy.

References

[1] See, e.g., Burroughes J H, Bradley D D C, Brown A R, Marks R N, Mackay K, Friend R H, Burns P L and Holmes A B 1990 *Nature* **347** 539

[2] Bumm L A, Arnold J J, Cygan M T, Dunbar T D, Burgin T P, Jones L, Allara D L, Tour J M and Weiss P S 1996 *Science* **272** 1323
Andres R P, Bein T, Dorogi M, Feng S, Henderson J I, Kubiak C P, Mahoney W, Osifchin R G and Reifenberger R 1996 *Science* **273** 1690

[3] Datta S, Tian W, Hong S H, Reifenberger R, Henderson J I and Kubiak C P 1997 *Phys. Rev. Lett.* **79** 2530

[4] Boulas C, Davidovits J V, Rondelez F and Vuillaume D 1996 *Phys. Rev. Lett.* **76** 4797

[5] Yazdani A, Eigler D M and Lang N D 1996 *Science* **272** 1921

[6] See, e.g., Conwell E M 1997 *Handbook of Organic Conductive Molecules and Polymers* vol 4, ed H S Nalwa (New York: Wiley)

[7] Joachim C and Vinuesa J F 1996 *Europhys. Lett.* **33** 635

[8] Datta S and Tian W 1997 *Phys. Rev.* B **55** R1914
[9] Samanta M P, Tian W, Datta S, Henderson J I and Kubiak C P 1996 *Phys. Rev.* B **53** R7626
[10] Yu Z G, Smith D L, Saxena A and Bishop A R 1997 *Phys. Rev.* B **56** 6494
Yu Z G, Smith D L, Saxena A and Bishop A R 1998 *J. Phys.: Condens. Matter* **10** 617
[11] Kadyshevitch A and Naaman R 1997 *Surf. Interface Anal.* **25** 71
Kadyshevitch A and Naaman R 1995 *Phys. Rev. Lett.* **74** 3443
[12] Haran A, Kadyshevitch A, Cohen H, Naaman R, Evans D, Seideman T and Nitzan A 1997 *Chem. Phys. Lett.* **268** 475
[13] Heeger A J, Kivelson S, Schreiffer J R and Su W P 1988 *Rev. Mod. Phys.* **60** 781